

# Channel Shaping Using Reconfigurable Intelligent Surfaces: From Diagonal to Beyond

Yang Zhao, *Member, IEEE*, Hongyu Li, *Graduate Student Member, IEEE*,  
Yijie Mao, *Member, IEEE*, Shanpu Shen, *Member, IEEE*, and Bruno Clerckx, *Fellow, IEEE*

## I. ASSUMPTION

We introduce Beyond-Diagonal (BD) Reconfigurable Intelligent Surface (RIS) in Multiple-Input Multiple-Output (MIMO) Point-to-point Channel (PC) and Interference Channel (IC). All proposals are based on assumption of *asymmetric* passive BD RIS, i.e., symmetry constraint  $\Theta_g = \Theta_g^T$  is relaxed. This is feasible when asymmetric passive components (e.g., ring hybrids and branch-line hybrids) [1] are available. This assumption was also made in Hongyu's papers [2], [3]. For quadratic problems, the proposed algorithms may be extended to symmetric BD RIS by replacing singular value decomposition with Takagi factorization [4].

## II. MIMO-PC

### A. Channel Power Maximization

Consider a BD RIS with  $N^S$  elements, which is divided into  $G$  groups of equal  $L$  elements.

$$\max_{\Theta} \left\| \mathbf{H}^D + \sum_g \mathbf{H}_g^B \Theta_g \mathbf{H}_g^F \right\|_F^2 \quad (1a)$$

$$\text{s.t.} \quad \Theta_g^H \Theta_g = \mathbf{I}, \quad \forall g \in \mathcal{G} \triangleq \{1, \dots, G\}. \quad (1b)$$

For *symmetric* BD-RIS, the problem has been solved in

- Matteo's paper [5]: SISO and equivalent<sup>1</sup>;
- Ignacio's paper [6]: SISO and directless MISO/SIMO.

**Remark 1.** The difficulty of (1) is that the RIS needs to balance the additive (direct-indirect) and multiplicative (forward-backward) eigenspace alignment. Interestingly, it has the same form as the weighted orthogonal Procrustes problem [7]:

$$\min_{\Theta} \left\| \mathbf{C} - \mathbf{A} \Theta \mathbf{B} \right\|_F^2 \quad (2a)$$

$$\text{s.t.} \quad \Theta^H \Theta = \mathbf{I}. \quad (2b)$$

There exists no trivial solution to (2). One lossy transformation, by moving  $\Theta$  to one side [8], formulates a standard orthogonal Procrustes problem:

$$\min_{\Theta} \left\| \mathbf{A}^\dagger \mathbf{C} - \Theta \mathbf{B} \right\|_F^2 \quad (3a)$$

$$\text{s.t.} \quad \Theta^H \Theta = \mathbf{I}. \quad (3b)$$

(3) has a global optimal solution  $\Theta^* = \mathbf{U} \mathbf{V}^H$ , where  $\mathbf{U}$  and  $\mathbf{V}$  are left and right singular matrix of  $\mathbf{A}^\dagger \mathbf{C} \mathbf{B}^H$  [9]. This low-complexity solution will be compared with the one proposed later.

<sup>1</sup>Single-stream MIMO with given precoder and combiner.

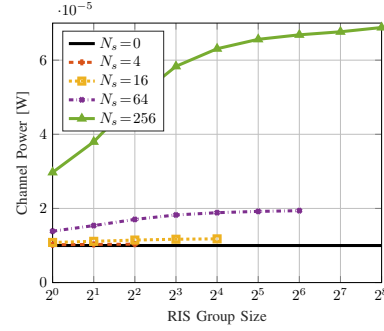


Fig. 1. Average channel power versus RIS elements  $N^S$  and group size  $L$ .  $(N^T, N^R) = (8, 4)$ ,  $(\Lambda^D, \Lambda^F, \Lambda^B) = (65, 54, 46)$  dB.

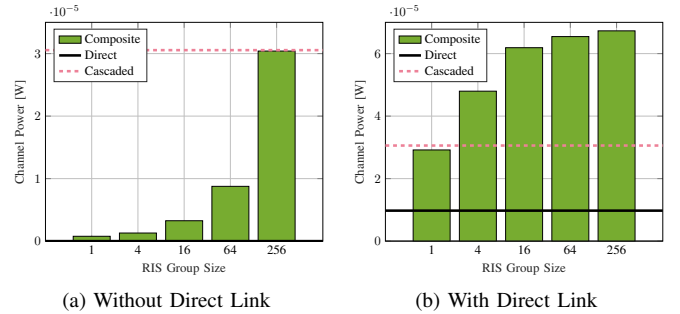


Fig. 2. Average channel power versus RIS group size  $L$ .  $(N^T, N^S, N^R) = (8, 256, 4)$ ,  $(\Lambda^D, \Lambda^F, \Lambda^B) = (65, 54, 46)$  dB.

Inspired by [10], we propose an iterative algorithm to solve (1). The idea is to successively approximate the quadratic objective with a sequence of affine functions and solve the resulting subproblems in closed form.

**Proposition 1.** Start from any  $\Theta^{(0)}$ , the sequence

$$\Theta_g^{(r+1)} = \mathbf{U}_g^{(r)} \mathbf{V}_g^{(r)}, \quad \forall g \quad (4)$$

converges to a stationary point of (1), where  $\mathbf{U}_g^{(r)}$  and  $\mathbf{V}_g^{(r)}$  are left and right singular matrix of

$$\begin{aligned} \mathbf{M}_g^{(r)} = & \mathbf{H}_g^B \mathbf{H}^D \mathbf{H}_g^H + \sum_{g' < g} \mathbf{H}_{g'}^B \mathbf{H}_{g'}^H \Theta_{g'}^{(r+1)} \mathbf{H}_{g'}^F \mathbf{H}_{g'}^H \\ & + \sum_{g' \geq g} \mathbf{H}_{g'}^B \mathbf{H}_{g'}^H \Theta_{g'}^{(r)} \mathbf{H}_{g'}^F \mathbf{H}_{g'}^H. \end{aligned} \quad (5)$$

*Proof.* To be added.  $\square$

Fig. 1 shows that, apart from adding reflecting elements  $N^S$ , increasing the group size  $L$  also improves the channel

power. This behavior is more pronounced for a large RIS. For example, the gain of pairwise connection is 2.8 % for  $N^S = 16$  and 28 % for  $N^S = 256$ . It implies that the channel shaping capability of BD RIS scales with group size  $L$ .

Fig. 2b and 2a compare the average channel power without and with direct link. ‘‘Cascaded’’ means the sum of element-wise product of first  $N = \min(N^T, N^S, N^R)$  eigenvalues (i.e., element-wise power product) of the forward and backward channels. We observe that diagonal RIS wastes substantial cascaded power and struggles to align the direct-indirect eigenspace. When the direct link is absent, only 2.6 % of available power is utilized by diagonal RIS while 100 % power is recycled by fully-connected RIS. When the direct link is present, the proposed BD RIS design can balance the direct-indirect and forward-backward eigenspace alignment for an optimal channel boost. It is worth noting that, when  $L$  is sufficiently large, the composite channel power surpasses the power sum of direct and cascaded channels, thanks to the constructive *amplitude superposition* of direct and cascaded channels. This again emphasizes the advantage of in-group connection of BD RIS.

### B. Rate Maximization

The problem is formulated w.r.t. precoder (instead of transmit covariance matrix) for reference:

$$\max_{\mathbf{W}, \Theta} R = \log \det \left( \mathbf{I} + \frac{\mathbf{W}^H \mathbf{H}^H \mathbf{H} \mathbf{W}}{\eta} \right) \quad (6a)$$

$$\text{s.t.} \quad \|\mathbf{W}\|_F^2 \leq P, \quad (6b)$$

$$\Theta_g^H \Theta_g = \mathbf{I}, \quad \forall g. \quad (6c)$$

(6) is jointly non-convex and solved by Alternating Optimization (AO). For a given  $\Theta$ , the optimal precoder is given by

$$\mathbf{W}^* = \mathbf{V} \mathbf{S}^{*1/2}, \quad (7)$$

where  $\mathbf{V}$  is right singular matrix of  $\mathbf{H}$  and  $\mathbf{S}^*$  is a diagonal matrix of the water-filling power allocation. For a given  $\mathbf{W}$ , we update  $\Theta$  by Riemannian Conjugate Gradient (RCG) method along the geodesics [11].

**Remark 2.** A geodesic refers to the shortest path between two points in a Riemannian manifold. Unitary constraint (6c) translates to a Stiefel manifold where the geodesics have simple expressions described by the exponential map [12].

For general optimization problems with block unitary constraint, the adapted RCG method at iteration  $r$  for block  $g$  is summarized below, where  $f(\Theta_g^{(r)})$  is the objective function also evaluated over  $\{\{\Theta_{g'}^{(r+1)}\}_{g' < g}, \{\Theta_{g'}^{(r)}\}_{g' > g}\}$ .

- 1) Compute the Euclidean gradient

$$\nabla_g^{\text{E}(r)} = \frac{\partial f(\Theta_g^{(r)})}{\partial \Theta_g^*}; \quad (8)$$

- 2) Translate to the Riemannian gradient

$$\nabla_g^{\text{R}(r)} = \nabla_g^{\text{E}(r)} \Theta_g^{(r)H} - \Theta_g^{(r)} \nabla_g^{\text{E}(r)H}; \quad (9)$$

### Algorithm 1: RCG Method for RIS MIMO-PC Rate Maximization

**Input:**  $\mathbf{H}^D, \mathbf{H}^F, \mathbf{H}^B, \mathbf{W}, L, \eta$

**Output:**  $\Theta^*$

```

1:  $r \leftarrow 0, \Theta^{(0)}$ 
2: Repeat
3:    $r \leftarrow r + 1$ 
4:   For  $g \leftarrow 1$  to  $G$ 
5:      $\Theta_g^{(r)} \leftarrow (14), (9)-(13)$ 
6:   End For
7: Until  $|R^{(r)} - R^{(r-1)}|/R^{(r-1)} \leq \epsilon$ 

```

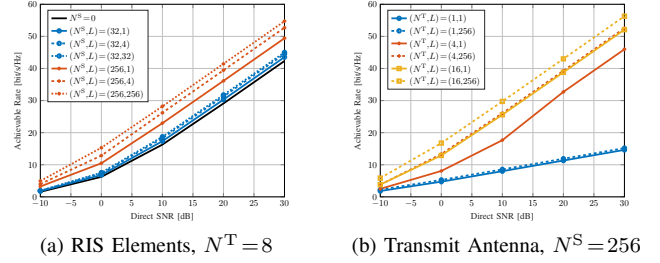


Fig. 3. Average achievable rate versus group size  $L$ .  $N^R = 4$ ,  $(A^D, A^F, A^B) = (65, 54, 46)$  dB.

- 3) Determine the weight factor

$$\gamma_g^{(r)} = \frac{\text{tr} \left( (\nabla_g^{\text{R}(r)} - \nabla_g^{\text{R}(r-1)}) \nabla_g^{\text{R}(r)H} \right)}{\text{tr} \left( \nabla_g^{\text{R}(r-1)} \nabla_g^{\text{R}(r-1)H} \right)}; \quad (10)$$

- 4) Compute the conjugate direction

$$\mathbf{D}_g^{(r)} = \nabla_g^{\text{R}(r)} + \gamma_g^{(r)} \mathbf{D}_g^{(r-1)}; \quad (11)$$

- 5) Determine the Armijo step size<sup>2</sup>

$$\mu_g^{(r)} = \arg \max_{\mu_g} f \left( \exp(\mu_g \mathbf{D}_g^{(r)}) \Theta_g^{(r)} \right); \quad (12)$$

- 6) Perform rotational update along local geodesics

$$\Theta_g^{(r+1)} = \exp \left( \mu_g^{(r)} \mathbf{D}_g^{(r)} \right) \Theta_g^{(r)}. \quad (13)$$

**Remark 3.** The adapted RCG method leverages the fact that block unitary matrices are closed under multiplication (but not necessarily under addition). Its advantage over universal manifold optimization [13], [14] is trifold:

- No retraction is involved;
- Lower computational complexity per iteration [12];
- Faster convergence thanks appropriate operational space.

The complex derivative of (6a) w.r.t. RIS block  $g$  is

$$\frac{\partial R}{\partial \Theta_g^*} = \frac{1}{\eta} \mathbf{H}_g^B H \mathbf{W} \left( \mathbf{I} + \frac{\mathbf{W}^H \mathbf{H}^H \mathbf{H} \mathbf{W}}{\eta} \right)^{-1} \mathbf{W}^H \mathbf{H}_g^F H. \quad (14)$$

Algorithm 1 summarizes the adapted RCG method for the RIS rate maximization subproblem.

Fig. 3a illustrates how RIS configuration influences the MIMO PC achievable rate. To ensure a 20 bit/s/Hz transmission, an Signal-to-Noise Ratio (SNR) of 13.5 dB is required for

<sup>2</sup>To double the step size, simply square the argument instead of recomputing the matrix exponential, i.e.,  $\exp(2\mu_g \mathbf{D}_g) = \exp^2(\mu_g \mathbf{D}_g)$ .

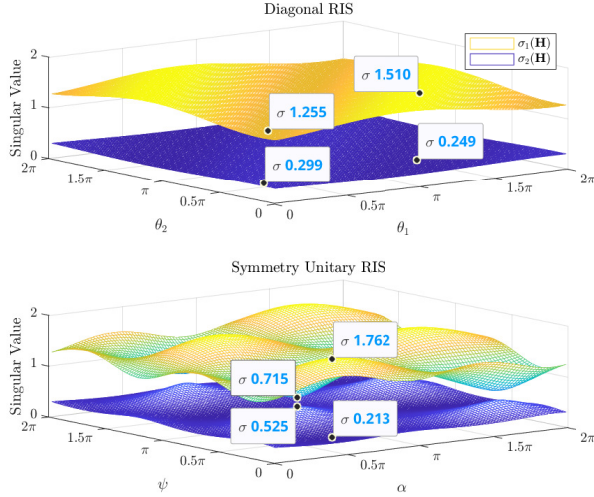


Fig. 4. Channel singular value shaping by diagonal and symmetry unitary RIS.  $(N^T, N^S, N^R) = (2, 2, 2)$ . Direct link is absent.

a 8T4R system. This value decreases to 12.5 dB (resp. 8 dB) when 32- (resp. 256-) element diagonal RIS is present. If tetrads can be formed in BD RIS, the SNR can be reduced by another 20 % (resp. 44 %). Further increase in  $L$  yields a marginal gain and incurs  $\mathcal{O}(L^2)$  connections. We thus conclude dyadic or tetradic BD RIS usually strike a good balance between performance and complexity.

### C. Channel Singular Value Redistribution

We first show the channel shaping benefit of BD RIS by a toy example. Consider  $(N^T, N^S, N^R) = (2, 2, 2)$  and assume the direct link is absent. The diagonal RIS is  $\Theta^D = \text{diag}(e^{j\theta_1}, e^{j\theta_2})$  while the unitary RIS has 4 independent angular parameters

$$\Theta^U = e^{j\phi} \begin{bmatrix} e^{j\alpha} \cos \psi & e^{j\beta} \sin \psi \\ -e^{-j\beta} \sin \psi & e^{-j\alpha} \cos \psi \end{bmatrix}. \quad (15)$$

When the direct link is absent,  $\phi$  has no impact on the singular value because  $\text{sv}(e^{j\phi} \mathbf{A}) = \text{sv}(\mathbf{A})$ . For a fair comparison, we enforce symmetry with  $\beta = \pi/2$ . Fig. 4 illustrates all possible channel singular values achieved by diagonal and symmetry unitary RIS. Despite using the same number of elements and parameters, BD RIS provides much wider dynamic ranges of  $\sigma_1(\mathbf{H})$  and  $\sigma_2(\mathbf{H})$  than diagonal RIS. Larger gaps are expected when the symmetry constraint can be relaxed.

We then analyze the channel shaping *capability* of BD RIS under specific setups.

1) *Rank-Deficient Channel*: In rank-deficient channels, BD RIS  $\Theta^B$  cannot achieve a higher Degree of Freedom (DoF) than diagonal RIS  $\Theta^D$ . This is because  $\text{sv}(\Theta^B) = \text{sv}(\Theta^D) = 1$  and

$$\begin{aligned} \text{rank}(\mathbf{H}) &\leq \text{rank}(\mathbf{H}^D) + \text{rank}(\mathbf{H}^B \Theta \mathbf{H}^F) \\ &\leq \text{rank}(\mathbf{H}^D) + \min(\text{rank}(\mathbf{H}^B), \text{rank}(\Theta), \text{rank}(\mathbf{H}^F)). \end{aligned} \quad (16)$$

Note BD RIS can still provide a higher indirect SNR as shown in Fig. 1 and 2.

2) *Rank-1 Indirect Channel*: The indirect channel is rank-1 iff the forward or backward channel is rank-1. Let  $\mathbf{H}^F = \sigma^F \mathbf{u}^F \mathbf{v}^{FH}$  without loss of generality. In this case, the channel Gram matrix can be written as Hermitian-plus-rank-1:

$$\mathbf{G} \triangleq \mathbf{H} \mathbf{H}^H = \mathbf{Y} + \mathbf{z} \mathbf{z}^H, \quad (17)$$

where  $\mathbf{Y} \triangleq \mathbf{H}^D (\mathbf{I} - \mathbf{v}^F \mathbf{v}^{FH}) \mathbf{H}^D = \mathbf{T} \mathbf{T}^H$  and  $\mathbf{z} \triangleq \sigma^F \mathbf{H}^B \Theta \mathbf{u}^F + \mathbf{H}^D \mathbf{v}^F$ . Regardless of RIS size and structure<sup>3</sup>, its  $n$ -th ( $n \geq 2$ ) eigenvalues are bounded by the Cauchy interlacing formula [9]

$$\lambda_1(\mathbf{Y}) \geq \lambda_2(\mathbf{G}) \geq \lambda_2(\mathbf{Y}) \geq \dots \geq \lambda_{N-1}(\mathbf{Y}) \geq \lambda_N(\mathbf{G}) \geq \lambda_N(\mathbf{Y}). \quad (18)$$

The equivalent singular value inequality is

$$\sigma_1(\mathbf{T}) \geq \sigma_2(\mathbf{H}) \geq \sigma_2(\mathbf{T}) \geq \dots \geq \sigma_{N-1}(\mathbf{T}) \geq \sigma_N(\mathbf{H}) \geq \sigma_N(\mathbf{T}). \quad (19)$$

(19) implies that, if the indirect channel is rank-1, then the RIS can at most enlarge the  $n$ -th ( $n \geq 2$ ) channel singular value to the  $(n-1)$ -th singular value of  $\mathbf{T}$ . Note that the largest channel singular value is unbounded with a sufficiently large RIS.

3) *Fully-Connected RIS Without Direct Link*: Denote the singular value decomposition of forward / backward channels as  $\mathbf{H}^{B/F} = \mathbf{U}^{B/F} \Sigma^{B/F} \mathbf{V}^{B/FH}$ . The composite channel is

$$\mathbf{H} = \mathbf{H}^B \Theta \mathbf{H}^F = \mathbf{U}^B \Sigma^B \mathbf{X} \Sigma^F \mathbf{V}^{FH}, \quad (20)$$

where  $\mathbf{X} = \mathbf{V}^{BH} \Theta \mathbf{U}^F$ .

**Proposition 2.** In this case, the singular value bounds on  $\mathbf{H}$  are equivalent to the singular value bounds on  $\mathbf{B}\mathbf{F}$ , where  $\mathbf{B}$  and  $\mathbf{F}$  are arbitrary matrices with singular values  $\Sigma^B$  and  $\Sigma^F$ .

*Proof.* We first observe that singular value control problem can be solved w.r.t. unitary  $\mathbf{X}$  and retrieved by  $\Theta = \mathbf{V}^B \mathbf{X} \mathbf{U}^{FH}$ . Also,  $\text{sv}(\mathbf{U}^B \Sigma^B \mathbf{X} \Sigma^F \mathbf{V}^{FH}) = \text{sv}(\bar{\mathbf{U}}^B \Sigma^B \bar{\mathbf{V}}^{BH} \bar{\mathbf{U}}^F \Sigma^F \bar{\mathbf{V}}^{FH}) = \text{sv}(\mathbf{B}\mathbf{F})$  where  $\bar{\mathbf{U}}^{B/F}$  and  $\bar{\mathbf{V}}^{B/F}$  are arbitrary unitary matrices.  $\square$

The problem now becomes, given  $\Sigma^B$  and  $\Sigma^F$ , what can we say about the singular value of  $\mathbf{B}\mathbf{F}$ . One comprehensive answer is Horn's inequality [16]: for all admissible triples  $(I, J, K)$ ,

$$\prod_{k \in K} \sigma_k(\mathbf{B}\mathbf{F}) \leq \prod_{i \in I} \sigma_i(\mathbf{B}) \prod_{j \in J} \sigma_j(\mathbf{F}). \quad (21)$$

It gives upper bound on the largest singular value and lower bound on the smallest singular value:

$$\sigma_1(\mathbf{B}\mathbf{F}) \leq \sigma_1(\mathbf{B}) \sigma_1(\mathbf{F}) \quad (22)$$

$$\sigma_N(\mathbf{B}\mathbf{F}) \geq \sigma_N(\mathbf{B}) \sigma_N(\mathbf{F}). \quad (23)$$

Another useful result is introduced in [17]: for all  $p > 0$ ,

$$\sum_n \sigma_n^p(\mathbf{B}\mathbf{F}) \leq \sum_n \sigma_n^p(\mathbf{B}) \sigma_n^p(\mathbf{F}). \quad (24)$$

When  $p=2$ , it implies the channel energy is upper bounded by the sum of element-wise power product of the forward and backward channels, as illustrated in Fig. 2(a). Interestingly, (22)–(24) are simultaneously tight when  $\mathbf{X} = \mathbf{I}$  and  $\Theta = \mathbf{V}^B \mathbf{U}^{FH}$ .

<sup>3</sup>A similar conclusion was made for diagonal RIS in [15].

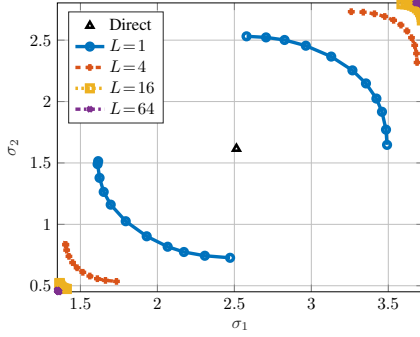


Fig. 5. Singular value Pareto front.  $(N^T, N^S, N^R) = (4, 64, 2)$ ,  $(A^D, A^F, A^B) = (0, -17.5, -17.5)$  dB.

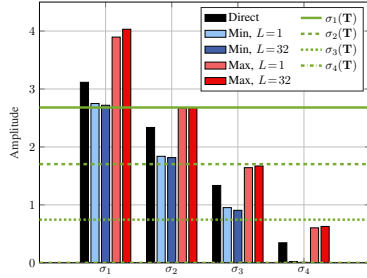


Fig. 6. Singular value bounds for rank-1 indirect channel.  $(N^T, N^S, N^R) = (4, 32, 4)$ ,  $(A^D, A^F, A^B) = (0, -17.5, -17.5)$  dB.

This solution was claimed in [18] to achieve channel capacity, but it is not true at moderate SNR.

Finally, we characterize the *Pareto front* of channel singular values via optimization approach.

$$\max_{\Theta} / \min_{\Theta} \quad J_1 = \sum_n \rho_n \sigma_n(\mathbf{H}) \quad (25a)$$

$$\text{s.t.} \quad \Theta_g^H \Theta_g = \mathbf{I}, \quad \forall g, \quad (25b)$$

where  $\rho_n$  is the weight of  $n$ -th singular value. The complex derivative of (25a) w.r.t. RIS block  $g$  is

$$\frac{\partial J_1}{\partial \Theta_g^*} = \mathbf{H}_g^B \mathbf{H}_g^H \mathbf{U} \text{diag}(\boldsymbol{\rho}) \mathbf{V}^H \mathbf{H}_g^F, \quad (26)$$

where  $\mathbf{U}$  and  $\mathbf{V}$  are left and right singular matrix of  $\mathbf{H}$ . (25) can be solved by RCG Algorithm 1 with (14) replaced by (26).

The Pareto front and evolving trend of channel singular values are shown in Fig. 5 and 6. Clearly, BD RIS with a larger group size can redistribute the channel singular values to a wider range.

### III. MIMO-IC

#### A. Leakage Interference Minimization

$$\min_{\Theta, \{\mathbf{G}_k\}, \{\mathbf{W}_k\}} \sum_{j \neq k} \sum \|\mathbf{G}_k (\mathbf{H}_{kj}^D + \mathbf{H}_k^B \Theta \mathbf{H}_j^F) \mathbf{W}_j\|_F^2 \quad (27a)$$

$$\text{s.t.} \quad \Theta_g^H \Theta_g = \mathbf{I}, \quad \forall g, \quad (27b)$$

$$\mathbf{G}_k \mathbf{G}_k^H = \mathbf{I}, \quad \mathbf{W}_k^H \mathbf{W}_k = \mathbf{I}, \quad \forall k. \quad (27c)$$

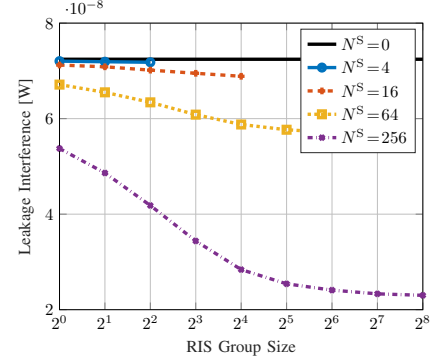


Fig. 7. Average leakage interference versus RIS elements  $N^S$  and group size  $L$ . Transmitters and receivers are randomly generated in a disk of radius 50 m centered at the RIS.  $(N^T, N^R, N^E, K) = (8, 4, 3, 5)$ ,  $(\gamma^D, \gamma^F, \gamma^B) = (3, 2.4, 2.4)$ , and reference pathloss at 1 m is  $-30$  dB.

The non-convex problem can be solved by Block Coordinate Descent (BCD) method. For a given  $\Theta$ , it reduces to conventional linear beamforming problem, for which an iterative algorithm alternating between the original and reciprocal networks is proposed in [19], [20]. At iteration  $r$ , the combiner at receiver  $k$  is updated as

$$\mathbf{G}_k^{(r)} = \mathbf{U}_{k,N}^{(r-1)H}, \quad (28)$$

where  $\mathbf{U}_{k,N}^{(r-1)}$  is the eigenvectors corresponding to  $N$  smallest eigenvalues of interference covariance matrix  $\mathbf{Q}_k^{(r-1)} = \sum_{j \neq k} \mathbf{H}_{kj} \mathbf{W}_j^{(r-1)} \mathbf{W}_j^{(r-1)H} \mathbf{H}_{kj}^H$ . The precoder at transmitter  $j$  is updated as

$$\mathbf{W}_j^{(r)} = \bar{\mathbf{U}}_{j,N}^{(r)}, \quad (29)$$

where  $\bar{\mathbf{U}}_{j,N}^{(r)}$  corresponds to interference covariance matrix  $\bar{\mathbf{Q}}_j^{(r)} = \sum_{k \neq j} \mathbf{H}_{kj}^H \mathbf{G}_k^{(r)} \mathbf{G}_k^{(r)H} \mathbf{H}_{kj}$  in the reciprocal network. Once  $\{\mathbf{G}_k\}$  and  $\{\mathbf{W}_k\}$  are determined, we define  $\bar{\mathbf{H}}_{kj}^D \triangleq \mathbf{G}_k \mathbf{H}_{kj}^D \mathbf{W}_j$ ,  $\bar{\mathbf{H}}_k^B \triangleq \mathbf{G}_k \mathbf{H}_k^B$ , and  $\bar{\mathbf{H}}_j^F \triangleq \mathbf{H}_j^F \mathbf{W}_j$ . The BD RIS subproblem reduces to

$$\min_{\Theta} \sum_{j \neq k} \sum \|\bar{\mathbf{H}}_{kj}^D + \bar{\mathbf{H}}_k^B \Theta \bar{\mathbf{H}}_j^F\|_F^2 \quad (30a)$$

$$\text{s.t.} \quad \Theta_g^H \Theta_g = \mathbf{I}, \quad \forall g. \quad (30b)$$

**Proposition 3.** Start from any  $\Theta^{(0)}$ , the sequence

$$\Theta_g^{(r+1)} = \mathbf{U}_g^{(r)} \mathbf{V}_g^{(r)}, \quad \forall g \quad (31)$$

converges to a stationary point of (30), where  $\mathbf{U}_g^{(r)}$  and  $\mathbf{V}_g^{(r)}$  are left and right singular matrix of

$$\mathbf{M}_g^{(r)} = \sum_{j \neq k} \sum (\mathbf{B}_{k,g} \Theta_g^{(r)} \mathbf{H}_{j,g}^F - \mathbf{H}_{k,g}^B \mathbf{H}_{k,j}^D \mathbf{D}_{k,j}^{(r)}) \mathbf{H}_{j,g}^F, \quad (32)$$

where  $\mathbf{B}_{k,g} = \lambda_1(\mathbf{H}_{k,g}^B \mathbf{H}_{k,g}^H) \mathbf{I} - \mathbf{H}_{k,g}^B \mathbf{H}_{k,g}^H$  and

$$\mathbf{D}_{k,j}^{(r)} = \mathbf{H}_{j,k}^D + \sum_{g' < g} \mathbf{H}_{k,g'}^B \mathbf{H}_{k,g'}^H \Theta_{g'}^{(r+1)} \mathbf{H}_{k,g'}^F + \sum_{g' > g} \mathbf{H}_{k,g'}^B \mathbf{H}_{k,g'}^H \Theta_{g'}^{(r)} \mathbf{H}_{k,g'}^F. \quad (33)$$

*Proof.* To be added.  $\square$



Fig. 7 illustrates how BD RIS helps to reduce the leakage interference. In this case, a fully-connected  $2^n$ -element BD RIS is almost as good as a diagonal  $2^{n+2}$ -element RIS in terms of leakage interference. Interestingly, the result suggests that BD RIS can achieve a higher DoF than diagonal RIS in MIMO-IC, which is not the case in MIMO-PC (as discussed in II-C1).

### B. Weighted Sum-Rate Maximization

$$\max_{\Theta, \{\mathbf{W}_k\}} J_2 = \sum_k \rho_k \log \det \left( \mathbf{I} + \mathbf{W}_k \mathbf{H}_{kj}^H \mathbf{Q}_k^{-1} \mathbf{H}_{kj} \mathbf{W}_k \right) \quad (34a)$$

$$\text{s.t.} \quad \Theta_g^H \Theta_g = \mathbf{I}, \quad \forall g, \quad (34b)$$

$$\|\mathbf{W}_k\|_F^2 \leq P_k, \quad \forall k \quad (34c)$$

where  $\rho_k$  is the weight of user  $k$  and  $\mathbf{Q}_k$  is the interference-plus-noise covariance matrix

$$\mathbf{Q}_k = \sum_{j \neq k} \mathbf{H}_{kj} \mathbf{W}_j \mathbf{W}_j^H \mathbf{H}_{kj}^H + \eta \mathbf{I}. \quad (35)$$

For a given  $\Theta$ , (34) reduces to conventional linear beamforming problem, for which a closed-form iterative solution based on Weighted Sum-Rate (WSR)-Weighted MMSE (WMMSE) relationship is proposed in [21]. At iteration  $r$ , the Minimum Mean-Square Error (MMSE) combiner at receiver  $k$  is

$$\mathbf{G}_k^{(r)} = \mathbf{W}_k^{(r-1)H} \mathbf{H}_{kk}^H (\mathbf{Q}_k^{(r-1)} + \mathbf{H}_{kk} \mathbf{W}_k^{(r-1)} \mathbf{W}_k^{(r-1)H} \mathbf{H}_{kk}^H)^{-1}, \quad (36)$$

the corresponding error matrix is

$$\mathbf{E}_k^{(r)} = (\mathbf{I} + \mathbf{W}_k^{(r-1)H} \mathbf{H}_{kk}^H \mathbf{Q}_k^{(r-1)} \mathbf{H}_{kk} \mathbf{W}_k^{(r-1)})^{-1}, \quad (37)$$

the Mean-Square Error (MSE) weight is

$$\Omega_k^{(r)} = \rho_k \mathbf{E}_k^{(r)-1}, \quad (38)$$

the Lagrange multiplier is

$$\lambda_k^{(r)} = \frac{\text{tr}(\eta \Omega_k^{(r)} \mathbf{G}_k^{(r)} \mathbf{G}_k^{(r)H} + \sum_j \Omega_k^{(r)} \mathbf{T}_{kj}^{(r)} \mathbf{T}_{kj}^{(r)H} - \Omega_k^{(r)} \mathbf{T}_{jk}^{(r)} \mathbf{T}_{jk}^{(r)H})}{P_k}, \quad (39)$$

where  $\mathbf{T}_{kj}^{(r)} = \mathbf{G}_k^{(r)} \mathbf{H}_{kj} \mathbf{W}_j^{(r)}$ . The precoder at transmitter  $k$  is

$$\mathbf{W}_k^{(r)} = \left( \sum_j \mathbf{H}_{jk}^H \mathbf{G}_j^{(r)H} \Omega_k^{(r)} \mathbf{G}_j^{(r)} \mathbf{H}_{jk} + \lambda_k^{(r)} \mathbf{I} \right)^{-1} \mathbf{H}_{kk}^H \mathbf{G}_j^{(r)H} \Omega_k^{(r)}. \quad (40)$$

Once  $\{\mathbf{W}_k\}$  is determined, the complex derivative of (34a) w.r.t. RIS block  $g$  is

$$\begin{aligned} \frac{\partial J_2}{\partial \Theta_g^*} &= \sum_k \rho_k \mathbf{H}_{k,g}^H \mathbf{Q}_k^{-1} \mathbf{H}_{kk} \mathbf{W}_k \mathbf{E}_k \mathbf{W}_k^H \\ &\quad \times (\mathbf{H}_{k,g}^H - \mathbf{H}_{kk}^H \mathbf{Q}_k^{-1} \sum_{j \neq k} \mathbf{H}_{kj} \mathbf{W}_j \mathbf{W}_j^H \mathbf{H}_{j,g}^H). \end{aligned} \quad (41)$$

The RIS subproblem can be solved by RCG Algorithm 1 with (14) replaced by (41).

A new observation from Fig. 8 that the interference alignment capability of BD RIS scales much faster with group size than number of elements.<sup>4</sup>

<sup>4</sup>The results are not very stable and depend heavily on initialization.

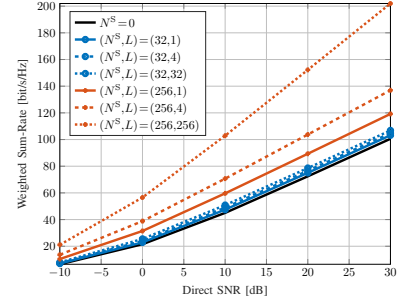


Fig. 8. Average weighted sum-rate versus SNR, RIS elements  $N^S$  and group size  $L$ .  $(N^T, N^R, N^E, K) = (8, 4, 3, 5)$ ,  $(A^D, A^F, A^B) = (65, 54, 46)$  dB,  $\rho_k = 1, \forall k$ .

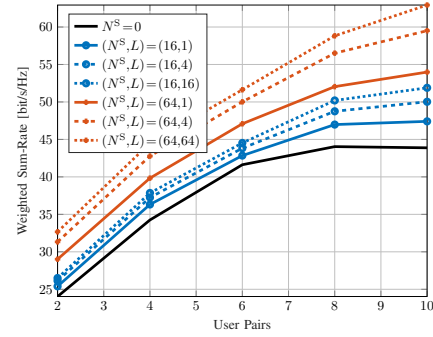


Fig. 9. Average weighted sum-rate versus user pairs  $K$ , RIS elements  $N^S$  and group size  $L$  at SNR = 15 dB.  $(N^T, N^R, N^E) = (4, 4, 3)$ ,  $\rho_k = 1, \forall k$ .

### REFERENCES

- [1] H.-R. Ahn, *Asymmetric Passive Components in Microwave Integrated Circuits*. Wiley, 2006. [Online]. Available: <https://books.google.co.uk/books?id=X6WdLbOuSNQC>
- [2] H. Li, S. Shen, and B. Clerckx, "Beyond diagonal reconfigurable intelligent surfaces: From transmitting and reflecting modes to single-, group-, and fully-connected architectures," *IEEE Transactions on Wireless Communications*, vol. 22, pp. 2311–2324, 4 2023.
- , "Beyond diagonal reconfigurable intelligent surfaces: A multi-sector mode enabling highly directional full-space wireless coverage," *IEEE Journal on Selected Areas in Communications*, vol. 41, pp. 2446–2460, 8 2023.
- [4] R. A. Horn and C. R. Johnson, *Matrix Analysis*. Cambridge University Press, 2012. [Online]. Available: <https://books.google.co.uk/books?id=O7sgAwAAQBAJ>
- [5] M. Nerini, S. Shen, and B. Clerckx, "Closed-form global optimization of beyond diagonal reconfigurable intelligent surfaces," *IEEE Transactions on Wireless Communications*, pp. 1–1, 2023. [Online]. Available: <https://ieeexplore.ieee.org/document/10155675/>
- [6] I. Santamaria, M. Soleymani, E. Jorswieck, and J. Gutiérrez, "Snr maximization in beyond diagonal ris-assisted single and multiple antenna links," *IEEE Signal Processing Letters*, vol. 30, pp. 923–926, 2023. [Online]. Available: <https://ieeexplore.ieee.org/document/10187688/>
- [7] J. C. Gower and G. B. Dijkstra, *Procrustes Problems*. OUP Oxford, 2004. [Online]. Available: <https://books.google.co.uk/books?id=kRRREAAQBAJ>
- [8] T. Bell, "Global positioning system-based attitude determination and the orthogonal procrustes problem," *Journal of Guidance, Control, and Dynamics*, vol. 26, pp. 820–822, 9 2003. [Online]. Available: <https://arc.aiaa.org/doi/10.2514/2.5117>
- [9] G. H. Golub and C. F. V. Loan, *Matrix Computations*. Johns Hopkins University Press, 2013. [Online]. Available: <https://jhupbooks.press.jhu.edu/title/matrix-computations>
- [10] F. Nie, R. Zhang, and X. Li, "A generalized power iteration method for solving quadratic problem on the stiefel manifold," *Science China Information Sciences*, vol. 60, p. 112101, 11 2017. [Online]. Available: <http://link.springer.com/10.1007/s11432-016-9021-9>

- [11] T. Abrudan, J. Eriksson, and V. Koivunen, "Conjugate gradient algorithm for optimization under unitary matrix constraint," *Signal Processing*, vol. 89, pp. 1704–1714, 9 2009. [Online]. Available: <https://linkinghub.elsevier.com/retrieve/pii/S0165168409000814>
- [12] T. E. Abrudan, J. Eriksson, and V. Koivunen, "Steepest descent algorithms for optimization under unitary matrix constraint," *IEEE Transactions on Signal Processing*, vol. 56, pp. 1134–1147, 3 2008. [Online]. Available: <http://ieeexplore.ieee.org/document/4436033/>
- [13] P.-A. Absil, R. Mahony, and R. Sepulchre, *Optimization Algorithms on Matrix Manifolds*. Princeton University Press, 2009. [Online]. Available: <https://books.google.co.uk/books?id=NSQGQeLN3NcC>
- [14] C. Pan, G. Zhou, K. Zhi, S. Hong, T. Wu, Y. Pan, H. Ren, M. D. Renzo, A. L. Swindlehurst, R. Zhang, and A. Y. Zhang, "An overview of signal processing techniques for ris/firs-aided wireless systems," *IEEE Journal of Selected Topics in Signal Processing*, vol. 16, pp. 883–917, 8 2022. [Online]. Available: <https://ieeexplore.ieee.org/document/9847080/>
- [15] D. Semmler, M. Joham, and W. Utschick, "High snr analysis of ris-aided mimo broadcast channels," in *2023 IEEE 24th International Workshop on Signal Processing Advances in Wireless Communications (SPAWC)*. IEEE, 9 2023, pp. 221–225. [Online]. Available: <https://ieeexplore.ieee.org/document/10304487/>
- [16] R. Bhatia, "Linear algebra to quantum cohomology: The story of alfred horn's inequalities," *The American Mathematical Monthly*, vol. 108, pp. 289–318, 4 2001. [Online]. Available: <https://www.tandfonline.com/doi/full/10.1080/00029890.2001.11919754>
- [17] L. Hogben, *Handbook of Linear Algebra*. CRC press, 2013.
- [18] G. Bartoli, A. Abrardo, N. Decarli, D. Dardari, and M. D. Renzo, "Spatial multiplexing in near field mimo channels with reconfigurable intelligent surfaces," *IET Signal Processing*, vol. 17, 3 2023. [Online]. Available: <https://ietresearch.onlinelibrary.wiley.com/doi/10.1049/sil2.12195>
- [19] K. Gomadam, V. R. Cadambe, and S. A. Jafar, "A distributed numerical approach to interference alignment and applications to wireless interference networks," *IEEE Transactions on Information Theory*, vol. 57, pp. 3309–3322, 6 2011. [Online]. Available: <http://ieeexplore.ieee.org/document/5773023/>
- [20] B. Clerckx and C. Oestges, *MIMO Wireless Networks: Channels, Techniques and Standards for Multi-Antenna, Multi-User and Multi-Cell Systems*. Elsevier Science, 2013. [Online]. Available: <https://books.google.co.uk/books?id=drEX1J7jHUIC>
- [21] F. Negro, S. P. Shenoy, I. Ghauri, and D. T. Slock, "Weighted sum rate maximization in the mimo interference channel." IEEE, 9 2010, pp. 684–689. [Online]. Available: <http://ieeexplore.ieee.org/document/5671658/>